Available online at www.sciencedirect.com

SCIENCE DIRECT®

Tectonophysics 386 (2004) 67–80

TECTONOPHYSICS

www.elsevier.com/locate/tecto

Why does the co-seismic slip of the 1999 Chi-Chi (Taiwan) earthquake increase progressively northwestward on the plane of rupture?

R. Cattin*, A. Loevenbruck, X. Le Pichon[1]

Laboratoire de Géologie, Ecole Normale Supérieure, 24 rue Lhomond, 75231 Paris Cedex 05, France

Received 18 July 2003; accepted 12 May 2004
Available online 17 July 2004

Abstract

The Chi-Chi 1999 earthquake ruptured the out-of-sequence Chelungpu Thrust Fault (CTF) in the fold-and-thrust belt in Western Central Taiwan. An important feature of this rupture is that the calculated slip increases approximately linearly in the SE–NW convergence plate direction from very little at its deeper edge to a maximum near the surface. We propose here a new explanation for this co-seismic slip distribution based on the study of both stress and displacement over the long-term as well as over a seismic cycle. Over the last 0.5 My, the convergence rate in the mountain front belt is accommodated by the frontal Changhua Fault (Ch.F), the CTF and the Shuangtung Fault (Sh.F). Based on previously published balanced cross sections, we estimate that the long-term slip of the Ch.F and of the CTF accommodate 5–30% and 30–55% of the convergence rate, respectively. This long-term partitioning of the convergence rate and the modeling of inter-seismic and post-seismic displacements suggest that the peculiar linear co-seismic slip distribution is accounted for by a combination of the effect of the obliquity of the CTF to the direction of inter-seismic loading, and of increasing aseismic creep on the deeper part of the Ch.F and CTF. Many previous interpretations of this slip distribution have been done including the effects of material properties, lubrication, site effect, fault geometry and dynamic waves. The importance of these processes with respect to the effects proposed here is still unknown. Taking into account the dip angle of the CTF, asperity dynamic models have been proposed to explain the general features of co-seismic slip distribution. In particular, recent works show the importance of heterogeneous spatial distribution of stress prior to the Chi-Chi earthquake. Our analysis of seismicity shows that previous large historic earthquakes cannot explain the amplitude of this heterogeneity. Based on our approach, we rather think that the high stress in the northern part of the CTF proposed by Oglesby and Day [Oglesby, D.D., Day, S.M., 2001. Fault geometry and the dynamics of the 1999 Chi-Chi (Taiwan) earthquake. Bull. Seismol. Soc. Am. 91, 1099–1111] reflects the latitudinal variation of inter-seismic coupling due to the obliquity of the CTF.

Keywords: Taiwan; Chi-Chi earthquake; Fault direction; Transition zone; Seismic cycle; Interseismic coupling

* Corresponding author. Fax: +33 1 44322000.
E-mail address: cattin@geologie.ens.fr (R. Cattin).
[1] Also at Collège de France, 6, place Marcelin-Berthelot, 75005 Paris, France.

0040-1951/$ - see front matter © 2004 Elsevier B.V. All rights reserved.
doi:10.1016/j.tecto.2004.05.002

1. Introduction

Taiwan Island extends along the convergent boundary between Philippine Sea Plate (PH) and Eurasia (EU) at the junction of the Manila and Ryukyu Trenches (Fig. 1). The rapid northwest motion of the Philippine Sea Plate (~80 mm/year) is accommodated by the eastward subduction of the South China Sea along the Manila Trench. To the north, beneath Taiwan Island, the Chinese margin underthrusts the Luzon volcanic arc in a subduction–collision process that is the cause of repeated large earthquakes within the fold-and-thrust belt in Western Taiwan (Fig. 1).

The most recent one is the 1999 Chi-Chi earthquake along the out-of-sequence Chelungpu Thrust

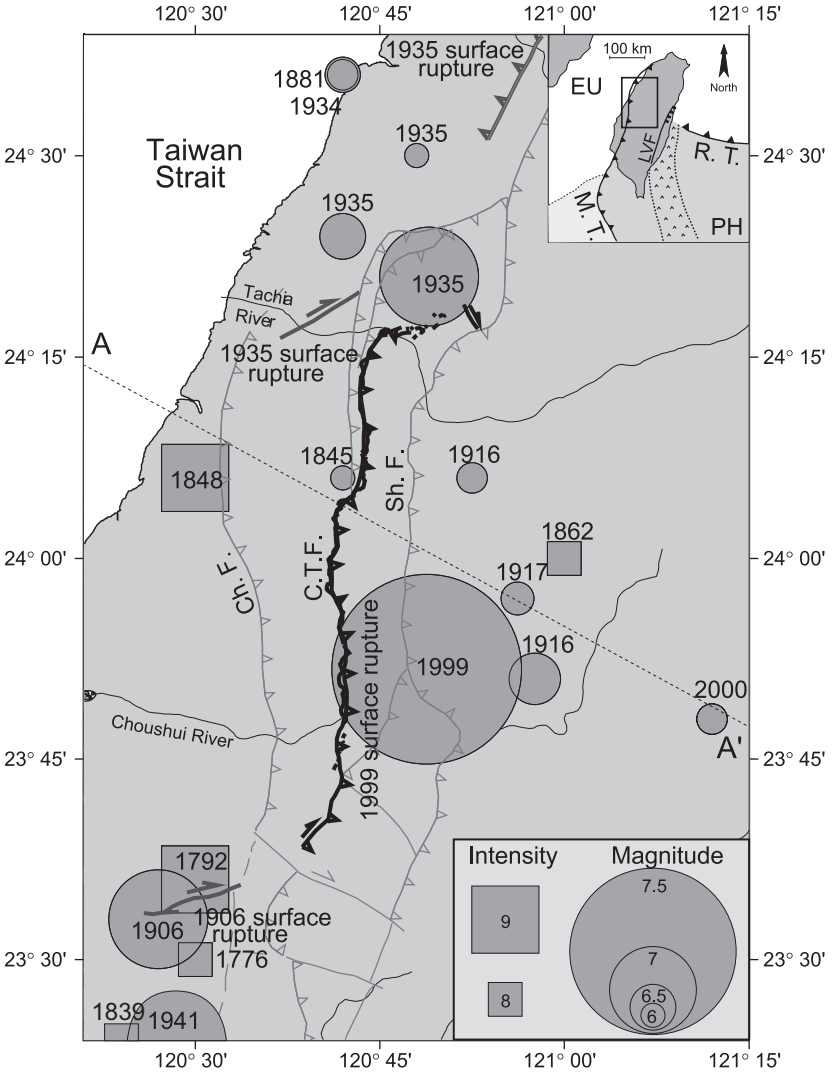

Fig. 1. Large historic earthquakes in Central Taiwan, 1776 to 2000 AD after Bonilla (1975), Tsai (1985), Wang and Wang (1993), Cheng et al. (1999) and NOAA data. Upper-right inset shows the regional geodynamic framework of Taiwan which extends along the convergent boundary between Philippine Sea Plate (PH) and Eurasia (EU) at the junction of the Manila (M.T.) and Ryukyu (R.T.) Trenches. Black line indicates the surface rupture of the main 20th century events (Meishan, 1906; Chihhu and Tuntzuchio, 1935; Chi-Chi, 1999). Faults: Ch.F., Changhua Fault, C.T.F. Chelungpu Thrust Fault, Sh.F., Shuangtung Fault. LVF: Longitudinal Valley Fault. Black dashed line AA′ gives the location of the N115° cross section discussed in this study.

Fault (CTF). The related co-seismic slip distribution is now well constrained (Fig. 2) by geological observations of the surface rupture, geodetic measurements (GPS and SPOT Satellite Images) as well as teleseismic and strong motion data (e.g. Johnson et al., 2001; Ma et al., 2001; Rubin et al., 2001; Dominguez et al., 2003; Loevenbruck et al., in press; Johnson and Segall, 2004). Modeling shows that the co-seismic rupture affects the ramp and the flat décollement of the CTF and does not extend to the Taiwan Main Detachment on which CTF is rooted (Carena et al., 2002). Whereas subduction earthquakes commonly

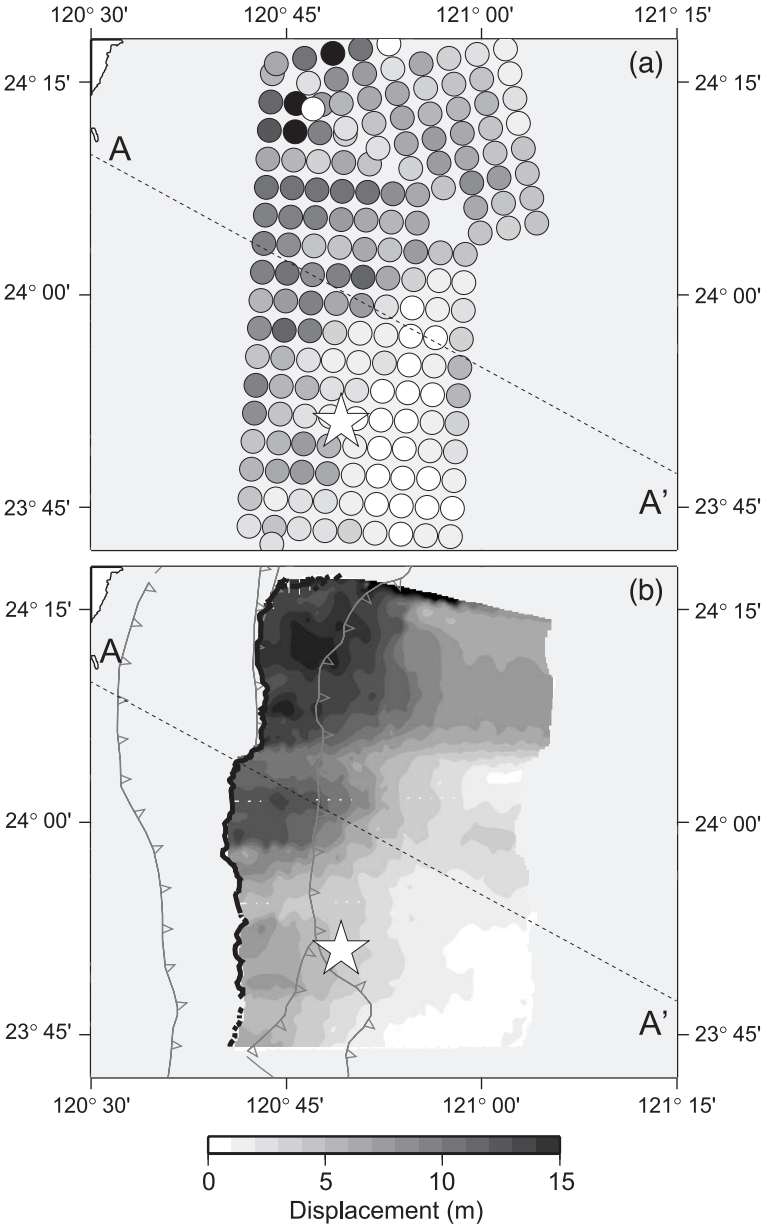

Fig. 2. Calculated co-seismic slip distribution obtained from (a) joint inversion of strong motion, teleseismic and GPS data (Ma et al., 2001) and (b) inversion of GPS and SPOT data (Loevenbruck et al., in press). The star gives the location of the mainshock.

generate larger slip amount at depth than along the shallow part of the seismogenic zone (e.g. Sagiya and Thatcher, 1999; Salichon et al., 2003), the calculated slip of the Chi-Chi earthquake increases northward and toward the surface where it reaches a maximum of about 15 m. Loevenbruck et al. (in press) show that a simple model defined by a linear increase of slip amount with convergence plate direction gives a good approximation of general features of the Chi-Chi co-seismic slip (Fig. 3). This pointed out the relationship between two different time scales: (1) the co-seismic slip and (2) the geological convergence rate between the Philippine Sea Plate and the Eurasia, which can be studied using the seismic cycle approach.

However the peculiar co-seismic slip distribution cannot be easily explained in terms of a simple stress release due to inter-seismic stress accumulation at the deeper edge of a fully locked seismogenic zone. First, the CTF is not an isolated fault. The frontal Changhua Fault (Ch.F) and the Shuangtung Fault (Sh.F) are also active structures of the fold-and-thrust belt and could accommodate part of the convergence. Second, the inter-seismic coupling of the CTF still remains to be quantified. Third, post-seismic measurements in the 15 months after the mainshock show significant displacements which can play a significant role in the seismic cycle.

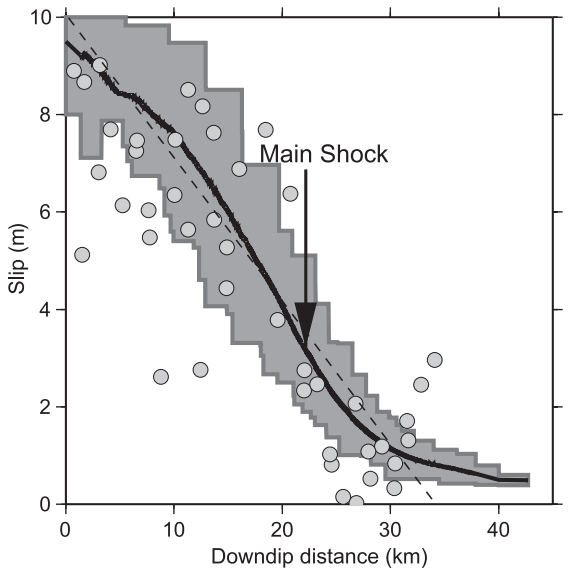

Fig. 3. Calculated co-seismic slip distribution along the CTF within a 15-km-wide swath along profile AA′ (see Fig. 2) showing a linear decrease with depth (dashed line). Zero and 43.2 km on the horizontal axis correspond to the surface and to the down-dip edge of the fault, respectively. Average slip (black line), lowest and highest slip (gray lines) obtained by Loevenbruck et al. (in press). Circles give the slip distribution obtained by Ma et al. (2001).

Hereafter, we address these features of the Chi-Chi earthquake assuming that the inter-seismic strain accumulation on the CTF is totally released by co-seismic and post-seismic displacements. In other words, the geological convergence rate is equivalent to the displacement rate over a complete seismic cycle. First, we quantify the contribution of each major frontal thrust (Ch.F, CTF and Sh.F) in the convergence rate across the collision belt over the last 0.5 My. Second, we examine the role of the inter-seismic and post-seismic displacements in the Chi-Chi earthquake slip distribution. We interpret the fault slip distribution in terms of (1) a thick transition zone between the upper locked portion and the lower ductile portion of the CTF, (2) the CTF obliquity to the plate convergence. Third, we discuss the previous interpretations to explain why the co-seismic slip increases northwestward on the plane rupture. Special emphasis is given to the analysis of the asperity dynamic model proposed by Oglesby and Day (2001) in the light of the stress effect of previous events. Finally, we discuss some general implications for seismic hazard assessment of thrust faulting in collision and subduction zones.

2. Kinematic behavior of the thrust and fold belt

2.1. Modeling approach

To examine the geologic–seismic cycle convergence rate, we first ignore the lateral variation of slip. We use the closed-form analytical expression obtained by Rani and Singh (1992) to calculate the surface displacements due to a two-dimensional dip–slip fault of finite width embedded in a uniform elastic half space. We consider a 500-km-long section in the direction of plate convergence through the Taiwan Island and Philippine Sea Plate (see Fig. 1 for location). Rani and Singh's formulation is modified in order to incorporate slip and dip angle variations along this profile. Following Suppe (1986), we consider the three major frontal thrust faults (Ch.F, CTF and Sh.F) which root into the nearly horizontal

Taiwan Main Detachment (TMD) that has been imaged at a depth of ~10 km (Carena et al., 2002). As Loevenbruck et al. (2001), we also consider the eastern part of Taiwan where the TMD steepens and may connect to the 45–50° east dipping Longitudinal Valley Fault (LVF). This geometry is used for both geologic rate and seismic cycle displacements.

2.2. Velocities over the last 0.5 My

We assume in the following that the present-day tectonic structure in western Taiwan exists at least since 0.5 My. This assumption seems to us reasonable as this age is the estimated age of the Ch.F in northern Pakuashan (Déramond et al., 1996).

From previously published retrodeformable cross sections, Lee et al. (2001) estimate an average long-term slip rate on the CTF of 10–15 mm/year during the last million years. Following the same approach but assuming that the CTF was initiated only about 0.7 million years ago, Chen et al. (2001) obtain an average slip rate of at least 17.1 mm/year.

The long-term slip rate along the Ch.F and Sh.F over the last 0.5 My is still unconstrained. Nevertheless, Mouthereau et al. (1996, 1999) use a detailed structural analysis and retrodeformable cross sections to obtain an average slip rate along the Ch.F ranging from 1 to 11 mm/year with an azimuth of N300°E close to the present-day azimuth of plate convergence. The analysis of stream gradient changes reveals that all frontal thrust faults, including the Sh.F, were active during the period 1904 to 1985 (Sung et al., 2000).

Thus, the Ch.F accommodates 1 to 11 mm/year (i.e. 15–30%) and the CTF 10 to 17 mm/year (i.e. 30–55%) of the long-term convergence rate (Fig. 4). We conclude that part of the shortening must be accommodated (seismically or not) along the Sh.F or by aseismic deformation within the fold-and-thrust belt.

2.3. Depth variations of inter-seismic coupling

Loevenbruck et al. (2001) interpret inter-seismic velocities as aseismic slip on a 10-km-deep décollement leading to strain accumulation on the locked CTF and on the partly locked Longitudinal Valley fault. This preliminary modeling has two obvious shortcomings. First, the deep edge of the fully locked CTF is not well constrained and second it does not take into account the CTF obliquity to the plate convergence. We address these two issues in the next paragraphs.

The increase of co-seismic slip toward the surface can be studied in terms of depth variations of the fully locked CTF. To address this question, we study the displacements during a seismic cycle along a 2D profile in the direction of the plate convergence located in the middle of the Chi-Chi rupture. We estimate the inter-seismic strain accumulation on the CTF assuming that over a complete seismic cycle it is totally released by co-seismic and post-seismic displacements. The post-seismic slip distribution obtained by Yu et al. (2003)

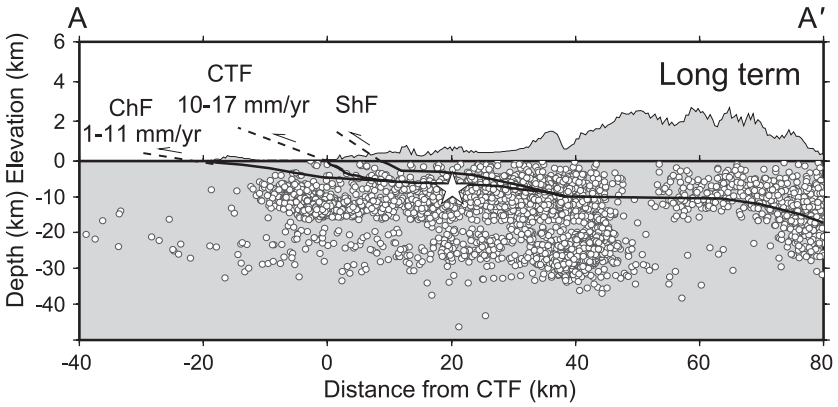

Fig. 4. Model of long-term (~0.5 My) deformation in Central Taiwan along profile AA′. Star gives the hypocentral location of Chi-Chi earthquake obtained by Chang et al. (2000). Long-term slip rate and geometry of major frontal thrust given by balanced cross-section and seismicity.

shows that 15 months after the earthquake, afterslip is concentrated south and down-dip of the largest co-seismic slip. The maximum post-seismic slip (45.9 cm) is located in the hypocentral region. There is little or no post-seismic slip in the area of maximum co-seismic slip. In contrast, significant slip (10 cm) occurs in the lower décollement below the seismogenic zone. Thus, we have calculated along our studied profile the total amount of slip associated with previous modeling (Loevenbruck et al., in press; Yu et al., 2003) of both co-seismic and post-seismic GPS displacements (Fig. 5(a)).

Using the estimated long-term velocities and previous studies (Loevenbruck et al., 2001; Domin-

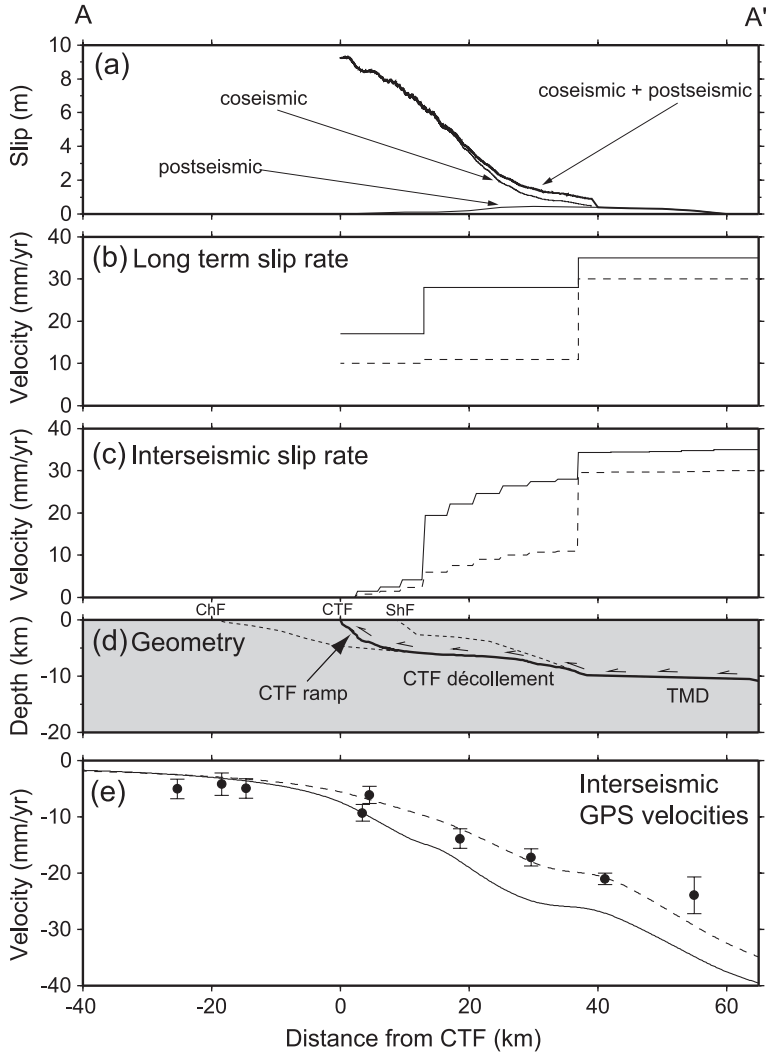

Fig. 5. Quantification of inter-seismic coupling along the profile AA′. (a) Total amount of co-seismic and post-seismic slip along the CTF and TMD obtained by Loevenbruck et al. (in press) and Yu et al. (2003). (b) Upper (black line) and lower (dashed line) bound of the long-term slip partitioning. (c) Estimated inter-seismic slip assuming that over a complete seismic cycle it is totally released by co-seismic and post-seismic displacements. Black and dashed lines give the maximum and the minimum inter-seismic slip, respectively. (d) Geometry of main thrust faults infers from surface geology, seismic reflection profile, wells and small earthquakes (Carena et al., 2002). (d) Calculated (black and dashed lines) and measured (Yu et al., 2001) (black circles) inter-seismic displacements.

guez et al., 2003), we quantify the contribution of each major fault in the convergence rate across Taiwan. The ~80 mm/year between Philippine Sea plate and Eurasia are accommodated along the Longitudinal Valley Fault (45–50 mm/year) and the 10-km-deep TMD (30–35mm/year). Fig. 5(b) shows that slip on the TMD is partitioned on the Sh.F (7–19 mm/year), the CTF décollement (11–28 mm/year), the CTF ramp (10–17 mm/year) and the Ch.F (1–11 mm/year).

Assuming that the CTF is unlocked at the down-dip edge of the co-seismic rupture, we obtain at the lower edge of the seismogenic zone an inter-seismic velocity v_{DE} ranging from 11 to 28 mm/year. Furthermore, assuming that the CTF is fully locked where the co-seismic slip is maximum we obtain a recurrence interval T for the Chi-Chi earthquake of 540 to 920 years. These values are consistent with the estimated age of the penultimate rupture on the northeastern segment of the CTF of 300–500 years (Lin et al., 2003) to 1400–2000 years (Ota et al., 2003).

We calculate the inter-seismic velocities on the CTF ramp

$$v_{inter} = v_{CTF} - u/T, \quad (1)$$

and along the CTF décollement

$$v_{inter} = v_{DE} - (u - u_{DE})/T, \quad (2)$$

where v_{CTF} is the long-term velocity on the CTF ramp (10–17 mm/year), u is the total amount of co-seismic and post-seismic displacement and u_{DE} is the co-seismic and post-seismic displacement at the down-dip edge of the co-seismic rupture. The estimated inter-seismic velocity is plotted in Fig. 5(c).

Based on elastic dislocation formulation (Rani and Singh, 1992), we calculate the surface velocities associated with the estimated inter-seismic velocities along the CTF and the TMD (Fig. 5(d)). The calculated inter-seismic velocities obtained with this assumption of no deformation after a complete seismic cycle are in good agreement with the GPS velocities (Yu et al., 2001) (Fig. 5(e)). As previously obtained (Loevenbruck et al., 2001), the upper edge of the CTF is fully locked and most of the shortening is accommodated along the 10-km-deep TDM (30–35 mm/year). However in contrast with our previous study, our new model shows that part of the CTF, including CTF ramp, may be unlocked.

Using the same dislocation approach, we calculate the co-seismic and post-seismic surface displacements along the profile AA′. Fig. 6 shows the good agreement between the measured (Yu et al., 2001, 2003; Dominguez et al., 2003) and calculated surface displacements. With this approach, we have a simple model that accounts for seismic cycle displacements and geometry of the CTF and TMD. We propose that the aseismic creep during inter-seismic period increases the strain accumulation toward the surface and thus explains a significant part of the linear increase of co-seismic slip in the convergence direction.

2.4. Effect of the obliquity of the CTF

In the area of the Chi-Chi earthquake, the geological structures, including the CTF, are not perpendicular to the plate convergence but present an obliquity of ~25° with the direction of convergence. To test the effect of this obliquity, we project the GPS inter-seismic velocities first along profiles in the direction of the fault trace of the CTF (N5°E) and second along profiles perpendicular to the plate convergence (N28.5°E) (see Fig. 7). To compare the influence of the obliquity along various profiles, we use the normalized inter-seismic velocity

$$v_{norm} = \frac{v}{v_{south}}, \quad (3)$$

where v is the velocity along a profile and v_{south} is the velocity at the southern edge of the same profile. Fig. 8 shows the weighted linear regression (large weight is applied to the southern velocity) of normalized inter-seismic velocity for both directions (N5°E and N28.5°E). Inter-seismic velocities in the southern part of profiles in the direction of the CTF are three times as large as in the northern part. In contrary, there is little change of the inter-seismic velocities with latitude along profiles perpendicular to the plate convergence. The increase with latitude of inter-seismic velocities due to the obliquity of the CTF could explain the increase of the co-seismic slip northward even in the absence of latitudinal variation of the long-term slip rate.

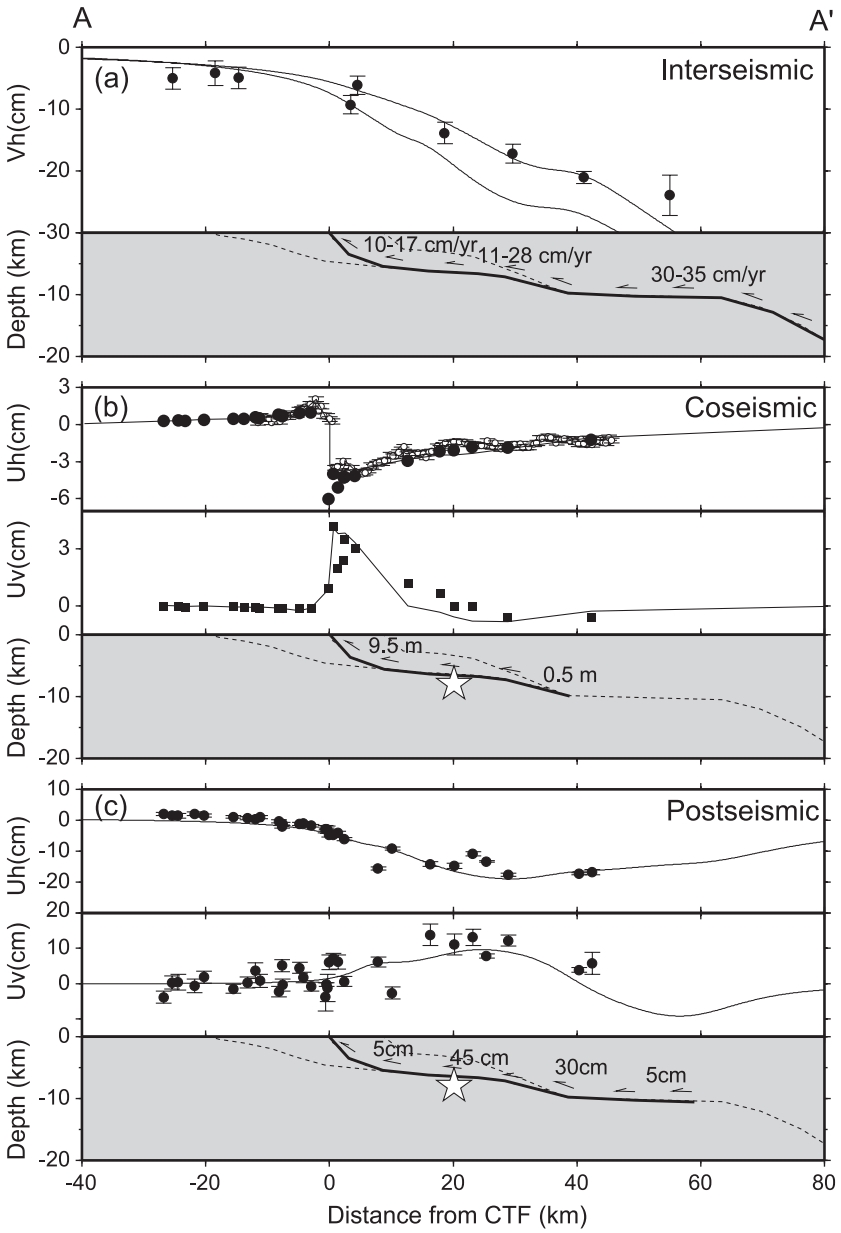

Fig. 6. Model of seismic cycle deformation in Central Taiwan along profile AA′. Star gives the hypocentral location of Chi-Chi earthquake obtained by Chang et al. (2000). (a) Calculated (black lines) and GPS (black circles) (Yu et al., 2001) inter-seismic horizontal velocities (Vh) and associated slip rates at depth. (b) Calculated horizontal (Uh) and vertical (Uv) co-seismic displacement. GPS horizontal (Yu et al., 2001) (black circles)—SPOT (Dominguez et al., 2003) (open circles) and GPS vertical Yu et al. (2001) (squares) displacements. (c) Calculated (black line) and GPS (Yu et al., 2003) (black circles) post-seismic horizontal (Uh) and vertical (Uv) displacements and associated slip at depth.

The linear inter-seismic slip decrease in the plate convergence direction and the obliquity of the fault relative to this trend imply lateral variations of both inter-seismic loading and co-seismic slip along the fault plane. With thrust faulting perpendicular to the plate convergence, the inter-seismic slip decreases

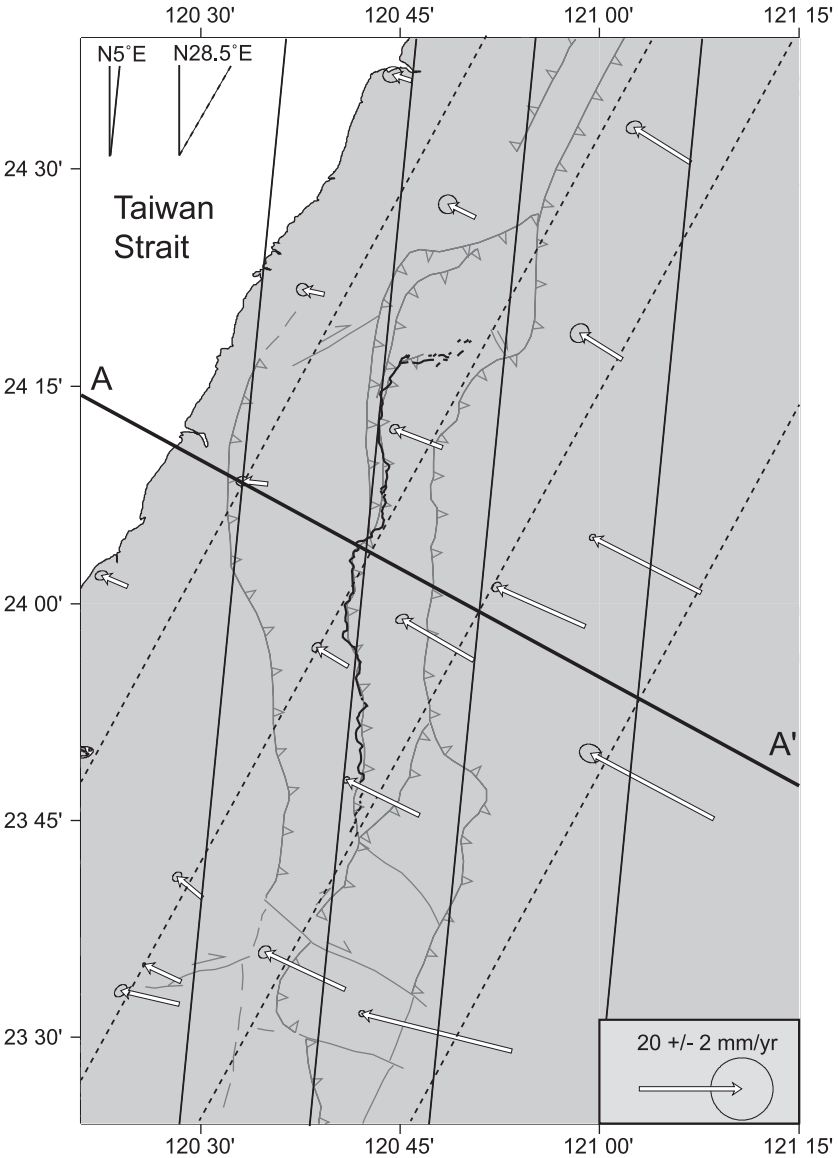

Fig. 7. Measured inter-seismic velocities (Yu et al., 2001) and profiles used to test the effect of the obliquity of the CTF. Black lines give the profiles used in the direction of the fault trace of the CTF (N5°E). Dashed lines give the profiles perpendicular to the plate convergence (N28.5°E).

linearly in the direction of convergence (Fig. 9a) and implies an increase of co-seismic slip upward (Fig. 9b). The obliquity of the fault during inter-seismic loading then implies that the associated co-seismic slip increases both upward and laterally (Fig. 9c and d). Hence, we propose that the Chi-Chi co-seismic slip distribution is the product of a combination of an upward increase of inter-seismic coupling and of a northwestward decrease of inter-seismic strain due to the obliquity of the CTF with the plate convergence. This simple approach is consistent with the recent results of Hsu et al. (2003) based on 2D dislocation model showing an increase of inter-seismic slip southward. However, our simple elastic model cannot

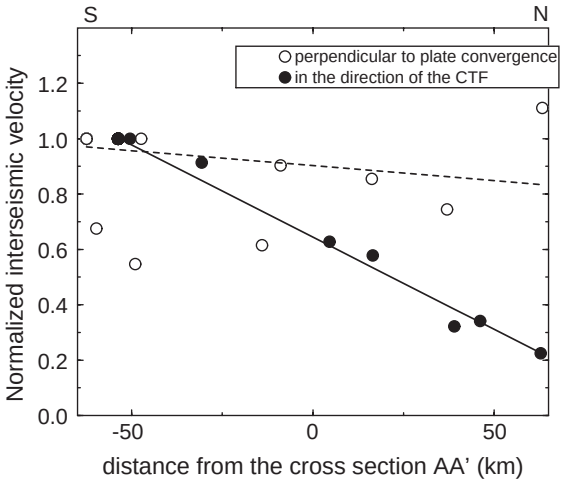

Fig. 8. Projected inter-seismic velocities showing the effect of the obliquity of the CTF to the plate convergence. Black and white circles are obtained from projection of inter-seismic velocities along profiles with an azimuth of N5°E (direction of the CTF) and N28.5°E (perpendicular to the plate convergence), respectively (see Fig. 7 for location). The normalized velocity is the ratio between the velocity along a profile and the velocity at the southern edge of the same profile. Black and dashed lines are obtained from the weighted linear regression of black and white circles, respectively. A large weight is applied to the southern normalized velocity.

be used for a complete analysis of both geological and seismic cycle displacement. Over a long time period, the deformation is clearly anelastic. Furthermore, there is no strong evidence that repeated earthquakes on the same fault have the same slip distribution. Following the approach of Cattin and Avouac (2000) in the Himalayas, more realistic two-dimensional finite element model should be developed to study the active mountain building processes and seismic cycle in Taiwan.

3. Discussion

3.1. Alternative explanations to our model

The combination of a thick transition zone and of the effect of the CTF obliquity proposed here may not be the unique factor to explain why the co-seismic slip increases northwestward. Other interpretations have been proposed. Ma et al. (2003) interpret both the increase of displacements and the decrease of acceleration northward as a lubrication effect. The low friction hypothesis is also proposed by Dominguez et al. (2003) to explain the co-seismic deformation locally in excess. Others propose that the increase of slip northward may be due to material properties. Locally, the increase of co-seismic slip could reflect a zone with very weak elastic parameters. Cattin et al. (1999) have shown that a decrease by about a factor 10 of the Young modulus can increase the horizontal displacements by up to 40%. In contrast, the decrease of the Young modulus has only a small effect on vertical displacements. We think that the increase of both vertical and horizontal displacements reflects anelastic properties (Seno, 2000).

The last set of interpretations is based on dynamic effects. Following previous theoretical studies (e.g. Brune, 1996; Oglesby et al., 2000), Oglesby and Day (2001) explain most of the general features of the co-seismic slip distribution of the Chi-Chi event with three-dimensional dynamic modeling of earthquakes. In this approach, the increase of co-seismic slip toward the surface is associated with the geometry of the CTF. The dip angle of the CTF allows radiated seismic waves to reflect off the free surface and to hit the fault again, increasing the co-seismic displacement toward the surface. In this model, the northward increase of slip is explained by a high-stress concentration zone in the northern part of the CTF. This circular zone has a radius of 16 km and is centered at 22 km down-dip and 25 km along strike from the northern end. At the center of this asperity, the increase of shear and normal stresses is 14.4 and 27 MPa, respectively. However, this approach does not take into account neither the site response (Seno, 2000) nor the geometric effect due to curvature of the northern part of the fault. Nevertheless, it gives a general conceptual framework to interpret the slip distribution of the Chi-Chi earthquake in term of heterogeneous spatial distribution of stress.

3.2. Stress effect of previous historic earthquakes

A simple explanation for such as heterogeneous stress distribution on the CTF before the Chi-Chi event could be the effect of previous earthquakes on and near the CTF (Fig. 1). To test this hypothesis, we calculate the stress change on the CTF due to previous

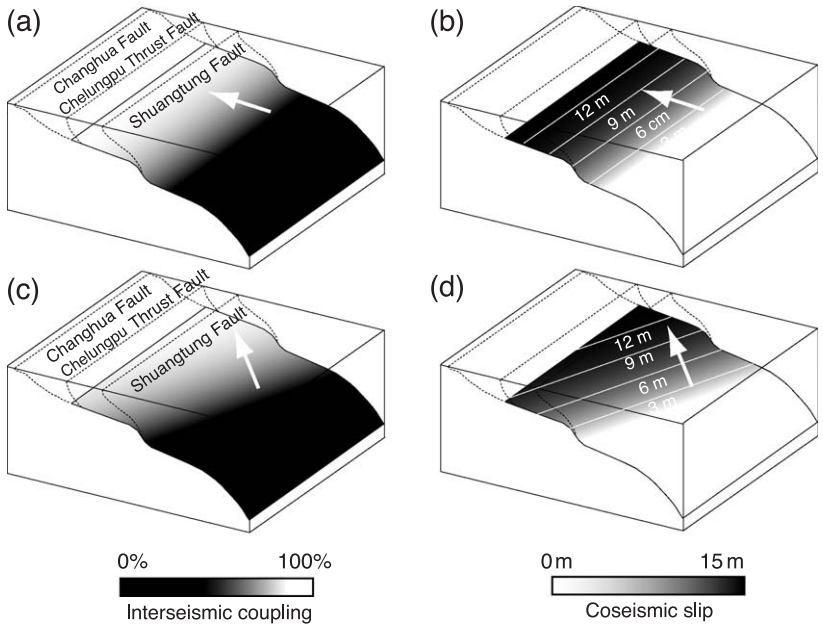

Fig. 9. Schematic diagram showing the conceptual effects of aseismic creep on the deeper part of the thrust faults in central Taiwan and of the obliquity of these structures to the direction of inter-seismic loading. White arrow gives the direction of the plate convergence. (a) Inter-seismic coupling with no obliquity. (b) Associated co-seismic slip with no obliquity. (c) Inter-seismic coupling with obliquity. (d) Associated co-seismic slip with obliquity.

historic earthquakes using the three-dimensional formulation of Okada (1992).

A few historical earthquakes (M<7) occurred on the CTF in 1845, 1862, 1916 and 1917, near the hypocentral location of the Chi-Chi event. But their locations (far from Chi-Chi rupture) and their small magnitudes (<6.5) cannot account for the formation of the asperity proposed by Oglesby and Day (2001). The 1906 Meishan earthquake with an oblique slip and a magnitude of 7.1 occurred on a 13-km-long fault (Bonilla, 1975). The maximum of slip was located on the eastern part of the fault, less than ~10 km away from the southern end of the Chi-Chi earthquake rupture. It consisted of a 2.4-m right-lateral slip and a 1.2-m dip–slip. The 1935 Chihhu and Tuntzuchio events occurred at the northern extremity of the 1999 rupture. The slip on the 15-km-long Chihhu fault consisted of <0.6-m right-lateral slip and 3-m dip–slip (Bonilla, 1975). For the Tuntzuchio earthquake, the rupture, approximately 12 km long, displayed right-lateral slip of as much as 1.5 m and maximum vertical displacement of 1 m. These two events were associated with secondary faulting in the same area.

We calculate the stress change on the CTF before the Chi-Chi earthquake due to these 1906 and 1935 events. We use a simple elastic dislocation modeling (Okada, 1992) with a homogeneous slip distribution given by the maximum of slip at the surface depicted above for both the 1906 and 1935 events. Fig. 10 shows that the shear stress change increases toward the surface and the normal stress change decreases northward. This stress distribution is then qualitatively in agreement with a co-seismic slip similar to the one observed for the Chi-Chi event. Nevertheless, the amplitudes of stress changes (<0.5 MPa) are much smaller than those in the asperity model proposed by Oglesby and Day (2001). This justifies a posteriori our previous assumption of not taking into account the smaller events. As mentioned by Oglesby and Day (2001), the parameters of the asperity such as its size and location are not well constrained by their analysis. One can argue that the historical record is limited (~200 years) compared to the estimated average time span between major earthquakes on the CTF (~1000 years). Thus, the amplitudes of stress changes could be increased by a factor 5. It is doubtful however that the heterogeneous prestress due

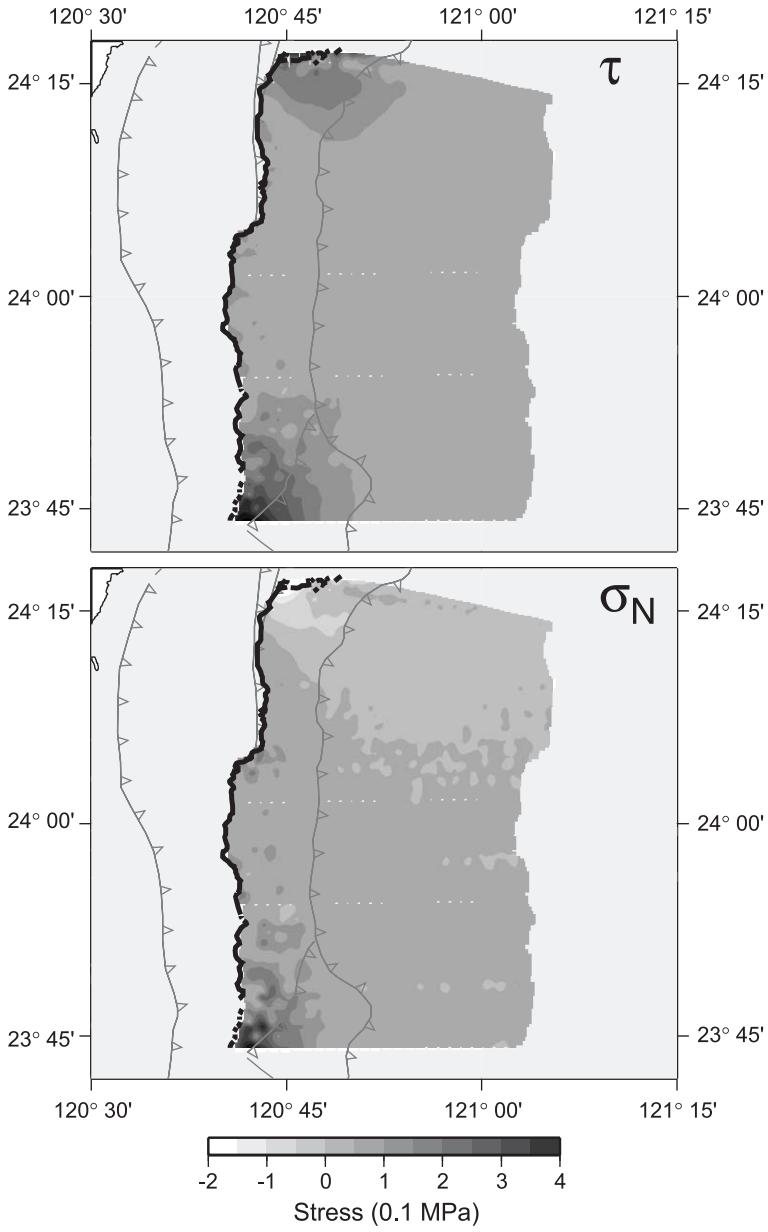

Fig. 10. Shear and normal stress change on the CTF due to the 1906 and 1935 earthquakes.

to previous earthquakes obtained in our study would fit their model. Based on our approach on the seismic cycle, we rather think that the high stress in the northern part of the CTF proposed by Oglesby and Day (2001) reflects the latitudinal variation of inter-seismic coupling due to the obliquity of the CTF.

4. Implications and conclusion

Our simple approach appears to reconcile all data on recent deformation in Taiwan (including both geological convergence rate and seismic cycle displacements) and the geometry of the thrust system

as constrained from surface geology, seismic reflection profile, wells and small earthquakes. During the inter-seismic period, the stress increases on frontal thrust faults (Ch.F, CTF and Sh.F) in the transition zone between a creeping lower décollement and a fully locked upper part. This upward increasing stress concentration cannot be compensated by the post-seismic displacements that play a significant role in the seismic cycle only on the deeper edge of the seismogenic zone. We show that a key part of the explanation of the upward stress build-up lies in the downward increasing aseismic strain during the inter-seismic phase. This result tends to support models similar to the one proposed by Rolandone and Jaupart (2002) with a thick transition zone between the upper locked portion and the ductile lower portion. In these models, the amount of ductile slip increases approximately linearly downward in the transition zone.

We wish to stress however that the seismic cycle in Taiwan is complex and cannot be studied only with our simple elastic approach. For instance, material properties and dynamic effects probably play a key role in explaining the features of the co-seismic slip distribution. Moreover, the study of seismic cycle on the Ch.F or Sh.F must now take into account the heterogeneity of the spatial stress distribution due to the Chi-Chi earthquake. One must further quantify the long-term slip and the average recurrence interval of earthquakes along all major frontal faults.

The study of the Nankai subduction zone has revealed the important role played by splay faults in the ruptures of large subduction earthquakes (Cummins and Kaneda, 2000). Following Seno (2000) and Lallemand (2000), the Chi-Chi earthquake can be regarded as the rupture of a splay fault within an active accretionary wedge. Assuming that the slip distribution of the Chi-Chi earthquake is a general feature of thrust faulting (Oglesby and Day, 2001) would have important implications as it implies the existence of large tsunamigenic earthquakes when the thrust faults are below water. First, major subduction earthquakes can occur along splay fault rather than along the interplate décollement. Second, the high dip angle of splay faults and the increase of slip toward the surface cause an enhanced uplift. Based on this approach, the same amount of seismic moment can generate a larger tsunami. In contrast to Seno (2000), we consider that the low dip angle of the focal mechanisms of tsunami earthquakes is compatible with this assumption if the splay fault has a ramp and flat geometry as the CTF.

Acknowledgements

R.C. is grateful to L. Bollinger and J.P. Avouac for insisting that he must understand co-seismic slip in terms of the seismic cycle in Taiwan as in their previous studies in Nepal. The manuscript has benefited from comments by Ya Ju Hsu, an anonymous reviewer and the associate editor Kevin Furlong. We are also grateful to Christel Tiberi for grammatical corrections of the manuscript. Most of the figures were made using the *GMT* software of Wessel and Smith.

References

Bonilla, M.G., 1975. A review of recently active faults in Taiwan. U.S. Geological Survey Open File Report 75-41, 58 pp.

Brune, J., 1996. Particle motions in a physical model of shallow angle thrust faulting. Proc. Indian Acad. Sci., A Earth Planet. Sci. 105, L197–L206.

Carena, S., Suppe, J., Kao, H., 2002. Active detachment of Taiwan illuminated by small earthquakes and its control of first-order topography. Geology 30, 935–938.

Cattin, R., Avouac, J.P., 2000. Modeling mountain building and the seismic cycle in the Himalaya of Nepal. J. Geophys. Res. 105, 13389–13407.

Cattin, R., Briole, P., Lyon-Caen, H., Bernard, P., Pinettes, P., 1999. Effects of superficials layers on coseismic displacements for a dip–slip fault and geophysical implications. Geophys. J. Int. 137, 149–158.

Chang, C.H., Wu, Y.M., Shin, T.C., Wang, C.Y., 2000. Relocation of the 1999 Chi-Chi earthquake in Taiwan. TAO 11, 581–590.

Chen, Y.G., Chen, W.S., Lee, J.C., Lee, Y.H., Lee, C.T., Chang, H.C., Lo, C.H., 2001. Surface rupture of the 1999 Chi-Chi earthquake yields insights on active tectonics of Central Taiwan. Bull. Seismol. Soc. Am. 91, 977–985.

Cheng, S.N., Yeh, Y.T., Hsu, M.T., Shin, T.C., 1999. Photo Album of Ten Disastrous Earthquakes in Taiwan, Published Jointly by the Central Weather Bureau and the Institute of Earth Sciences. Academia Sinica, Taipei, Taiwan.

Cummins, P.R., Kaneda, Y., 2000. Possible splay fault slip during the 1946 Nankai earthquake. Geophys. Res. Lett. 27, 2725–2728.

Déramond, J., Delcaillau, B., Souquet, P., Angelier, J., Chu, H.T., Lee, J.F., Lee, T.Q., Liew, P.M., Lin, T.S., Teng, L., 1996. Signatures de la surrection et de la subsidence dans les bassins

d'avant-chaîne actifs: les Foothills de Taiwan (de 8 Ma à l'Actuel). Bull. Soc. Géol. Fr. 167, 111–123.

Dominguez, S., Avouac, J.P., Michel, R., 2003. Horizontal coseismic deformation of the 1999 Chi-Chi earthquake measured from SPOT satellite images: implications for the seismic cycle along the western foothills of Central Taiwan. J. Geophys. Res. 108 (B2), 2083, doi:10.1029/2001JB000951.

Hsu, Y.J., Simons, M., Yu, S.B., Kuo, L.C., Chen, H.Y., 2003. A two-dimensional dislocation model for interseismic deformation of the Taiwan mountain belt. Earth Planet. Sci. Lett. 211, 287–294.

Johnson, K.M., Segall, P., 2004. Imaging the ramp-decollement geometry of the Chelungpu fault using coseismic GPS displacements from the 1999 Chi-Chi, Taiwan earthquake. Tectonophysics 378, 123–139.

Johnson, K.M., Hsu, Y.J., Segall, P., Yu, S.B., 2001. Fault geometry and slip distribution of the 1999 Chi-Chi, Taiwan earthquake imaged from inversion of GPS data. Geophys. Res. Lett. 28, 2285–2288.

Lallemand, S., 2000. Was the 1999 Chi-Chi earthquake in Taiwan a "Subduction Earthquake"? TAO 11, 709–720.

Lee, J.C., Chen, Y.G., Sieh, K., Mueller, K., Chen, W.S., Chu, H.T., Chan, Y.C., Rubin, C., Yeats, R., 2001. A vertical exposure of the 1999 surface rupture of the Chelungpu fault at Wufeng, Western Taiwan: structural and paleoseismic implications for an active thrust fault. Bull. Seismol. Soc. Am. 91, 914–929.

Lin, A., Chen, A., Ouchi, T., Maruyama, T., 2003. Geological evidence of Paleo-seismic events occurred along the Chelungpu fault zone, Taiwan. TAO 14, 13–26.

Loevenbruck, A., Cattin, R., Le Pichon, X., Courty, M.L., Yu, S.B., 2001. Seismic cycle in Taiwan derived from GPS measurements. C. R. Acad. Sci., II 333, 57–64.

Loevenbruck, A., Cattin, R., Le Pichon, X., Dominguez, S., Michel, R., in press. Coseismic slip resolution and post-seismic relaxation time of the 1999 Chi-Chi, Taiwan, earthquake as constrained by geological observations, geodetic measurements (GPS and SPOT satellite images) and seismicity data. Geophys. J. Int. 157 (3), 1415, doi:10.1111/j.1365-246X.2003.02373.x.

Ma, K.F., Mori, J., Lee, S.J., Yu, S.B., 2001. Spatial and temporal distribution of slip for the 1999 Chi-Chi, Taiwan, earthquake. Bull. Seismol. Soc. Am. 91, 1069–1087.

Ma, K.F., Brodsky, E.E., Mori, J., Ji, C., Song, T.R.A., Kanamori, H., 2003. Evidence for fault lubrication during the 1999 Chi-Chi, Taiwan, earthquake (Mw7.6). Geophys. Res. Lett. 30 (5), 1244, doi:10.1029/2002GL015380.

Mouthereau, F., Angelier, J., Deffontaines, B., Lacombe, O., Chu, H.T., Colletta, B., Déramond, J., Yu, M.S., Lee, J.F., 1996. Cinématique actuelle et récente du front de chaîne de Taiwan. C. R. Acad. Sci., II 323, 713–719.

Mouthereau, F., Lacombe, O., Deffontaines, B., Angelier, J., Chu, H.T., Lee, C.T., 1999. Quaternary transfer faulting and belt front deformation at Pakuashan (western Taiwan). Tectonics 18, 215–230.

Oglesby, D.D., Day, S.M., 2001. Fault geometry and the dynamics of the 1999 Chi-Chi (Taiwan) earthquake. Bull. Seismol. Soc. Am. 91, 1099–1111.

Oglesby, D.D., Archuleta, R.J., Nielsen, S.B., 2000. Dynamics of dip–slip faulting: explorations in two dimensions. J. Geophys. Res. 105, 13643–13653.

Okada, Y., 1992. Internal deformation due to shear and tensile faults in a half space. Bull. Seismol. Soc. Am. 82, 1018–1040.

Ota, Y., Shishikura, M., Watanabe, M., Sawa, H., Yamaguchi, M., Yanagida, M., Tanaka, T., Ichikawa, K., Lee, Y.H., Lu, S.T., Shih, T.S., 2003. Paleoseismology deduced from the Fengyan trench on the northern part of the Chelungpu Fault, central Taiwan: an example of very low angle reverse fault. EOS Trans. AGU, 84 (46) F1329.

Rani, S., Singh, S.J., 1992. Static deformation of a uniform half-space due to a long dip–slip fault. Geophys. J. Int. 109, 469–476.

Rolandone, F., Jaupart, C., 2002. The distribution of slip rate and ductile deformation in a strike-slip shear zone. J. Geophys. Res. 148, 179–192.

Rubin, C.M., Sieh, K., Chen, Y.G., Lee, J.C., Chu, H.T., Yeats, R., Mueller, K., Chan, Y.C., 2001. Surface rupture and behavior of thrust fault probed in Taiwan. EOS 82, 565–569.

Sagiya, T., Thatcher, W., 1999. Coseismic slip resolution along a plate boundary megathrust: the Nankai Through, southwest Japan. J. Geophys. Res. 104, 1111–1129.

Salichon, J., Delouis, B., Lundgren, P., Giardini, D., Costantini, M., Rosen, P., 2003. Joint inversion of broadband teleseismic and interferometric synthetic aperture radar (InSAR) data for the slip history of the Mw=7.7, Nazca ridge (Peru) earthquake of 12 November 1996. J. Geophys. Res. 108 (B2), 2085, doi:10.1029/2001JB000913.

Seno, T., 2000. The 21 September, 1999 Chi-Chi earthquake in Taiwan: implications for tsunami earthquakes. TAO 11, 701–708.

Sung, Q., Chen, Y.C., Tsai, H., Chen, Y.G., Chen, W.S., 2000. Comparison study of the coseismic deformation of the 1999 Chi-Chi earthquake and long term stream gradient changes along the Chelungpu fault in central Taiwan. TAO 11, 735–750.

Suppe, J., 1986. Reactivated normal faults in the western Taiwan fold-thrust belt. Mem. Geol. Soc. China 7, 187–200.

Tsai, Y.B., 1985. A study of disastrous earthquakes in Taiwan, 1683–1895. Earth. Sci. Bull. 5, 1–44.

Wang, C.T., Wang, J.H., 1993. Aspects of large Taiwan earthquakes and their aftershocks. TAO 4, 257–271.

Yu, S.B., Kuo, L.C., Hsu, Y.J., Su, H.H., Liu, C.C., Hou, C.S., Lee, J.F., Lai, T.C., Liu, C.C., Liu, C.L., Tseng, T.F., Tsai, C.S., Shin, T.C., 2001. Preseismic deformation and coseismic displacements associated with the 1999 Chi-Chi, Taiwan earthquake. Bull. Seismol. Soc. Am. 91, 995–1012.

Yu, S.B., Hsu, Y.J., Kuo, L.C., Chen, H.Y., 2003. GPS measurements of postseismic deformation following the 1999 Chi-Chi, Taiwan earthquake. J. Geophys. Res. 108, 2520.